Fisher information and quantum entropies of a 2D system under a pair of non-central scalar and vector potentials

A. Becir and M. Moumni

Laboratory of Radiations and Matter (PRIMALAB)
Department of Physics, Faculty of Science and Matter, University of Batna 1
e-mail: ahmed.becir@univ-batna.dz; m.moumni@univ-batna.dz

Received 14 March 2025; accepted 4 June 2025

In this study, we examine a 2 dimensional system influenced by a non-central potential consisting of a Kratzer potential with a dipole moment, along with a vector potential of the (AB) effect. We explore various information-theoretic measures, including Fisher information, Shannon entropy, Tsallis entropy, and Rényi entropy. Our numerical results show that the Fisher information increases with an increase in dissociation energy and decreases with rising dipole moment, Aharonov-Bohm potential strength, and both the radial and angular quantum numbers. In contrast, the Shannon entropy, the Tsallis entropy, and the Rényi entropy decrease with rising dissociation energy, while they increase with an increase in dipole moment, Aharonov-Bohm potential strength, as well as the principal and angular quantum numbers. These observations collectively indicate that the precision and localization of particles in space are enhanced by the increasing of the dissociation energy and reduced when the dipole moment, Aharonov-Bohm potential strength, and both the radial and angular quantum numbers increase.

Keywords: Fisher information; quantum entropies; non-central Kratzer potential; vector potential.

DOI: https://doi.org/10.31349/RevMexFis.71.061301

1. Introduction

Quantum information is the information of the state of a quantum system, and it combines principles from quantum mechanics and information theory to understand and manipulate information using quantum systems. Quantum information has some basic measures such as Rényi and Shannon entropies [1–3], Fisher information [4–7], Tsallis entropy [8–10], Fisher-Shannon complexity [11–13], and Cramér-Rao complexity [14].

Quantum information is a rapidly evolving field with the potential to cause revolutionary advances across various scientific and technological domains. Several researches have been conducted on studying the entropies and complexities of quantum systems. The position-and momentum-space entropies have been derived for various systems including the isotropic harmonic oscillator and the hydrogen atom in D dimensions [15–17], power-type potentials [18], central, Morse and Pöschl-Teller potentials [19,20], as well as Dirac-delta-like quantum potentials [21]. Furthermore, uncertainty relations have been verified for modified isotropic harmonic oscillators and Coulomb potentials in [22] and quantum information entropies and squeezing associated with the eigenstates of the isotonic oscillator have been discussed in [23].

Recent research has extended these investigations to encompass quantum information-entropic measures for half-line Coulomb potential [24], ring-shaped modified Kratzer potential [25], Pseudoharmonic Potential [26], Eckart Manning Rosen Potential [27], Shifted Tietz-Wei Potential [28], Hulthen-Kratzer potential [29], Generalized Morse potential [30], exponential-type potential [31], screened Kratzer potential [32], and for Eckart-Hellmann potential [33].

In this study, our focus lies in examining some quantum information measures to a two-dimensional system under the influence of a non-central Kratzer potential consisting of a Kratzer potential and a Dipole moment [34], alongside with a vector potential of the Aharonov-Bohm (AB) effect. The Kratzer potential is significant in depicting the internuclear vibrations observed in diatomic molecules [35]. Its relevance extends to the fields of molecular spectroscopy and quantum chemistry [36, 37] as well as to the investigation of optical properties in semiconductor quantum dots [38].

The interest in two-dimensional (2D) materials has grown significantly recently due to their unique properties and diverse applications in various fields. Graphene has been extensively developed for many electronic applications due to its electronic, thermal, optical and mechanical superiority [39]. It has exhibited potential in enhancing the performance of lithium-ion batteries by increasing their capacity [40] and has been employed in the fabrication of wind and solar cells [41]. Besides, graphene appears promising as a hydrogen storage material [42]. Black phosphorus (BP), another outstanding 2D material, has attracted attention due to its role as a layered semiconductor with a tunable bandgap and high carrier mobility. It is considered as one of the most promising candidates for numerous applications ranging from transistors, to photonics, optoelectronics, sensors, batteries, and catalysis [43, 44]. Moreover, transition metal dichalcogenides which are 2D materials have semiconducting properties and they have many applications in high-end electronics, spintronics, optoelectronics, energy harvesting, flexible electronics, DNA sequencing, and personalized medicine [45].

This paper is organized as follows: In Sec. 2 we solve the Schrödinger equation of a 2D system under the influence of a non-central potential composed of a Kratzer potential along with a dipole moment, as well as a vector potential from the Aharonov-Bohm (AB) effect, and find the energy eigenvalues and the corresponding normalized wave functions. Sections 3 and 4 are devoted to analytically deriving the Fisher information measure, Shannon, Tsallis, and Rényi entropies of the given system. In Sec. 5, we explore the impact of the dissociation energy, the dipole moment, the AB field, and the radial and angular quantum numbers on the derived quantum information measures, and subsequently discuss the obtained results. Finally, the last section provides a concise conclusion summarizing our findings.

2. The Exact solution of 2D Schrödinger equation with non-central scalar and vector potentials

The 2D Schrödinger equation for a system subjected to both a scalar potential and a vector potential of the Aharonov-Bohm (AB) effect, $\vec{\phi}_{AB}$ is written as [46]

$$\left[\frac{1}{2\mu}\left(i\hbar\vec{\nabla}+e\vec{\phi}_{AB}\right)^{2}+qV(r,\theta)\right]\psi(r,\theta)=E\psi(r,\theta): \quad \vec{\phi}_{AB}=\frac{\phi_{AB}}{2\pi r}\vec{e}_{\theta}. \tag{1}$$

Since the AB field satisfies the Coulomb gauge $\vec{\nabla}\cdot\vec{\phi}_{AB}=0$, then

$$\left(i\hbar\vec{\nabla}+e\vec{A}_{AB}\right)^{2}\psi(r,\theta)=\left(-\hbar^{2}\Delta+e^{2}A_{AB}^{2}+2ie\hbar\vec{A}_{AB}\cdot\vec{\nabla}\right)\psi(r,\theta), \tag{2}$$

and the Schrödinger Eq. (2) becomes

$$\left[-\frac{\hbar^{2}}{2\mu}\Delta+\frac{e^{2}\phi_{AB}^{2}}{8\pi^{2}\mu r^{2}}+i\frac{e\hbar\phi_{AB}}{2\mu\pi r^{2}}\frac{\partial}{\partial\theta}+V(r,\theta)\right]\psi(r,\theta)=E\psi(r,\theta). \tag{3}$$

The non-central potential studied in the article consists of two components: a modified Kratzer potential and an angular dipole moment [34]

$$V\left(r,\theta\right)=D_{e}\left(\frac{r-r_{e}}{r}\right)^{2}+\frac{D\cos\theta}{r^{2}}=\frac{A}{r}+\frac{B}{r^{2}}+C+\frac{D\cos\theta}{r^{2}}, \tag{4}$$

where $A=-2r_{e}D_{e}$, $B=r_{e}^{2}D_{e}$, $C=D_{e}$, D_{e} is the dissociation energy, which represents the energy required to completely separate the two atoms, r_{e} is the equilibrium bond length, which is the distance at which the potential energy is minimized, and D is the dipole moment.

Substituting (4) into (3) yields

$$\left[-\frac{\hbar^{2}}{2\mu}\Delta+\frac{e^{2}\phi_{AB}^{2}}{8\pi^{2}\mu r^{2}}+i\frac{e\hbar\phi_{AB}}{2\mu\pi r^{2}}\frac{\partial}{\partial\theta}+\left(\frac{A}{r}+\frac{B}{r^{2}}+\frac{D\cos\theta}{r^{2}}\right)\right]\psi(r,\theta)=(E-C)\psi(r,\theta). \tag{5}$$

If we let $E_{r}=2\mu\hbar^{-2}(E-C)$, $\gamma=B+(\hbar^{2}/2\mu)(\phi_{AB}^{2}/\phi_{0}^{2})$: $\phi_{0}=h/e$, then we get

$$\left[\frac{\partial^{2}}{\partial r^{2}}+\frac{1}{r}\frac{\partial}{\partial r}-\frac{2\mu}{\hbar^{2}}\frac{A}{r}-\frac{2\mu}{\hbar^{2}}\frac{\gamma}{r^{2}}+\frac{1}{r^{2}}\left(\frac{\partial^{2}}{\partial\theta^{2}}-2i\frac{\phi_{AB}}{\phi_{0}}\frac{\partial}{\partial\theta}-\frac{2\mu}{\hbar^{2}}D\cos\theta\right)\right]\psi=-E_{r}\psi. \tag{6}$$

Now making use of $\psi(r,\theta)=r^{-1/2}R(r)\Theta(\theta)$ the Eq. (6) can be decoupled into radial and angular parts

$$\left(\frac{d^{2}}{d\theta^{2}}-2i\frac{\phi_{AB}}{\phi_{0}}\frac{d}{d\theta}-\frac{2\mu}{\hbar^{2}}D\cos\theta\right)\Theta(\theta)=E_{\theta}\Theta(\theta), \tag{7}$$

$$\left(\frac{d^{2}}{dr^{2}}+\left(E_{\theta}+\frac{1}{4}-\frac{2\mu}{\hbar^{2}}\gamma\right)\frac{1}{r^{2}}-\frac{2\mu}{\hbar^{2}}\frac{A}{r}+E_{r}\right)R(r)=0. \tag{8}$$

Firstly, one needs to solve the angular Eq.(7) to determine the angular eigenvalue E_{θ}. Subsequently, this value should be substituted into the radial Eq. (8) to deduce the energy eigenvalue [34, 46]. By expressing the angular solution as $\Theta(\theta)=e^{i\delta\theta}\Phi(\theta)$, where $\delta=(\phi_{AB}/\phi_{0})$, and defining $\theta=2z$, $a=4\left(\delta^{2}-E_{\theta}\right)$, and $b=(4\mu/\hbar^{2})D$ the angular Eq. (7) transforms into the Mathieu equation.

$$\frac{\partial^{2}\Phi(z)}{\partial z^{2}}+(a-2b\cos 2z)\Phi(z)=0. \tag{9}$$

The differential Eq. (9) has periodic solutions of periods π or 2π, represented by the cosine-elliptic $ce_{2m}(z)$ and the sine-elliptic $se_{2m}(z)$ functions where m is a natural number [47]. If we keep the parameter b fixed, the Mathieu solutions are periodic only for specific values of the other parameter a. The latter parameter is called the characteristic number and is given for fractional m by [46, 48–50]

$$a_{2m}\approx 4m^{2}+\frac{1}{2l}b^{2}+\frac{20m^{2}+7}{32l^{3}(l-3)}b^{4}+\frac{36m^{4}+232m^{2}+29}{64l^{5}(l-3)(l-8)}b^{6}+\ldots,\quad \text{with } l=4m^{2}-1. \tag{10}$$

The phase factor $\exp(\imath\delta\theta)$ in $\Theta(\theta)$ arising from the Aharonov-Bohm (AB) field induces a shift in the angular quantum number m to $m+\delta$ [46, 51]. Consequently, the corresponding angular eigenvalue becomes

$$E_{\theta}^{m,\delta} = \delta^2 - \frac{1}{4} ce_{2(m+\delta)}\left(4\mu D/\hbar^2\right). \tag{11}$$

Now, considering the asymptote limits for the radial Eq. (8), the radial eigenfunction can be expressed as $R(r) = r^{\lambda}e^{-\beta r}f(r)$. Substituting this expression into Eq. (8), it becomes:

$$\left(r\frac{d^2}{dr^2} + 2\left(\lambda - \beta r\right)\frac{d}{dr} - 2\left(\frac{\mu A}{\hbar^2} + \lambda\beta\right)\right) f(r) = 0. \tag{12}$$

In deriving Eq. (12), we eliminated the coefficients of the terms involving r and $\frac{1}{r}$, knowing that β and λ are free parameters. This was achieved by setting

$$\beta = \sqrt{-E_r} = \sqrt{-\frac{2\mu}{\hbar^2}(E-C)}, \tag{13}$$

$$\lambda = \frac{1}{2} + \sqrt{-E_{\theta}^{(m,\delta)} + \frac{2\mu}{\hbar^2}\gamma} = \frac{1}{2} + \sqrt{-E_{\theta}^{(m,\delta)} + \frac{2\mu}{\hbar^2}B + \frac{\phi_{AB}^2}{\phi_0^2}}. \tag{14}$$

By defining $x = 2\beta r$, the differential Eq. (12) is transformed to confluent hypergeometric equation

$$\left(x\frac{d^2}{dx^2} + (2\lambda - x)\frac{d}{dx} - \left(\frac{\mu A}{\hbar^2\beta} + \lambda\right)\right) f(x) = 0, \tag{15}$$

with solutions

$$f(x) = \mathcal{N}{}_1F_1\left(-n_r, 2\lambda, x\right), \tag{16}$$

where $-n_r = (\mu A/\hbar^2\beta) + \lambda$ is the condition of quantization obtained from the asymptotic behavior of the confluent series ($r \to \infty \Rightarrow {}_1F_1 = 0$).

The wavefunction of the system is then given by

$$\psi(r,\theta) = \mathcal{N}e^{i\delta\theta}r^{\lambda-\frac{1}{2}}e^{-\beta r}\Phi(\theta){}_1F_1\left(-n_r, 2\lambda, 2\beta r\right), \tag{17}$$

with energy eigenvalues

$$E_{n_r,m} = -\frac{1}{2}\left[\sqrt{\frac{\hbar^2}{\mu}}\frac{1}{A}\left(n_r + \frac{1}{2} + \sqrt{-E_{\theta}^{(m,\delta)} + \frac{2\mu}{\hbar^2}B + \frac{\phi_{AB}^2}{\phi_0^2}}\right)\right]^{-2}. \tag{18}$$

The wavefunction (17) can be rewritten in term of Laguerre polynomials as

$$\psi(x,\theta) = Nx^{\lambda-\frac{1}{2}}e^{-\frac{x}{2}}e^{i\delta\theta}\Phi(\theta)L_{n_r}^{2\lambda-1}\left(x\right), \quad \text{with} \quad x = 2\beta r, \tag{19}$$

with the normalization constant

$$N = \sqrt{\frac{2\beta^2 n!}{(n+2\lambda-1)!(n+\lambda)\pi}}, \tag{20}$$

where we have used the fact that [52]

$$L_n^{\lambda-1}(x) \sim {}_1F_1\left(-n, \lambda, x\right). \tag{21}$$

3. Fisher information and Shannon entropy

3.1. Fisher information

Fisher information is a method for quantifying the extent of information that an observable random variable X provides regarding an unknown parameter θ, and it has many applications in statistics and information theory [53, 54]. It primarily focuses on capturing local variations within the density function. The Fisher information measure is formally defined as follows [55]

$$I(\rho) = \int \frac{\left(\vec{\nabla}\rho(\vec{r})\right)^2}{\rho(\vec{r})}\, d\vec{r}. \tag{22}$$

In 2D dimension, taking the gradient operator in polar coordinates $\vec{\nabla} = ([\partial/\partial r], [1/r][\partial/\partial\theta])$, the expression for the Fisher information is as follows

$$I(\rho) = \int \frac{1}{\rho(\vec{r})}\left[\frac{\partial\rho(\vec{r})}{\partial r}\right]^2 d\vec{r} + \int \frac{1}{\rho(\vec{r})}\left[\frac{\partial\rho(\vec{r})}{r\partial\theta}\right]^2 d\vec{r} \equiv I_1 + I_2, \tag{23}$$

where $\rho(\vec{r}) \equiv \rho(r,\theta) = |\psi(r,\theta)|^2$ is the probability density. Using the wave function (19) along with the normalization constant (20), the probability density is expressed as

$$\rho(r,\theta) = N^2 x^{2\lambda-1} e^{-x} \Phi^2(\theta)[L_n^{2\lambda-1}(x)]^2, \quad \text{with} \quad x = 2\beta r. \tag{24}$$

The derivative in the Eq. (23) yields

$$\begin{aligned}\frac{\partial\rho(r,\theta)}{\partial r} &= 2\beta N_r \Phi^2(\theta)\frac{\partial}{\partial x}\left(x^{2\lambda-1}e^{-x}[L_n^{2\lambda-1}(x)]^2\right)\\ &= 2\beta N^2\Phi^2(\theta)x^{2\lambda-1}e^{-x}\left[\left(\frac{2\lambda-1}{x}-1\right)[L_n^{2\lambda-1}(x)]^2 - 2L_n^{2\lambda-1}(x)L_{n-1}^{2\lambda}(x)\right],\end{aligned} \tag{25}$$

so that

$$\begin{aligned}I_1 &= \int_0^\infty\int_0^{2\pi} \frac{1}{\rho(r,\theta)}\left[\frac{\partial\rho(r,\theta)}{\partial r}\right]^2 r\,dr\,d\theta = \pi N^2\int_0^\infty x^{2\lambda}e^{-x}\left[\left(\frac{2\lambda-1}{x}-1\right)L_n^{2\lambda-1}(x) - 2L_{n-1}^{2\lambda}(x)\right]^2 dx\\ &= \frac{2\beta^2}{n+\lambda}\left[4n-(2\lambda-1)\right] + 4\beta^2,\end{aligned} \tag{26}$$

where we have used the fact that $\int_0^{2\pi}\Phi^2(\theta)\,d\theta = \pi$ and the relation [56]

$$\begin{aligned}\int_0^\infty x^{\alpha+\beta}e^{-x}\left[L_n^\alpha(x)\right]^2 dx = \frac{\Gamma(\alpha+n+1)}{\Gamma(n+1)}\sum_{k=0}^{n}(-1)^k\frac{\Gamma(n-k-\beta)}{\Gamma(-k-\beta)}\\ \times\frac{\Gamma(\alpha+k+\beta+1)}{\Gamma(\alpha+k+1)}\frac{1}{\Gamma(k+1)\Gamma(n-k+1)} \quad \text{with } \mathrm{Re}(\alpha+\beta+1) > 1.\end{aligned} \tag{27}$$

The second integral in Eq. (23) involves the following integral

$$\int_0^{2\pi}\frac{1}{\Phi^2(\theta)}\left[\frac{\partial\Phi^2(\theta)}{\partial\theta}\right]^2 d\theta = 4\int_0^{2\pi}\left[\frac{\partial\Phi(\theta)}{\partial\theta}\right]^2 d\theta = 4m^2\pi. \tag{28}$$

Computing the integral (28) is straightforward if the characteristic number $b = 0$. For $b \neq 0$, it is also easy to check that this integral tends to $4m^2\pi$ for any values of m.

Using the result (28), the second integral in Eq. (23) becomes

$$I_2 = 4\pi m^2 N^2\int_0^\infty x^{2\lambda-2}e^{-x}[L_n^{2\lambda-1}(x)]^2\,dx = \frac{8m^2\beta^2}{(n+\lambda)(2\lambda-1)}. \tag{29}$$

Therefore, the Fisher information is given by

$$I(\rho) = I_1 + I_2 = \frac{2\beta^2}{(n+\lambda)}\left[4n + \frac{4m^2}{2\lambda-1} - (2\lambda-1)\right] + 4\beta^2. \tag{30}$$

It is worth noting that, in the evaluation of quantum information measures such as Fisher information, and Shannon, Tsallis, and Rényi entropies, it is standard practice to integrate over the entire physical domain of the wavefunction, *i.e.*, from 0 to ∞ in radial coordinates. Although the wavefunction (19) decays exponentially with factor $e^{-\beta r}$, its probability density is nonzero all over the way to infinity. Therefore, integrating over the full spatial range is essential in order to obtain results that are accurate and physically consistent.

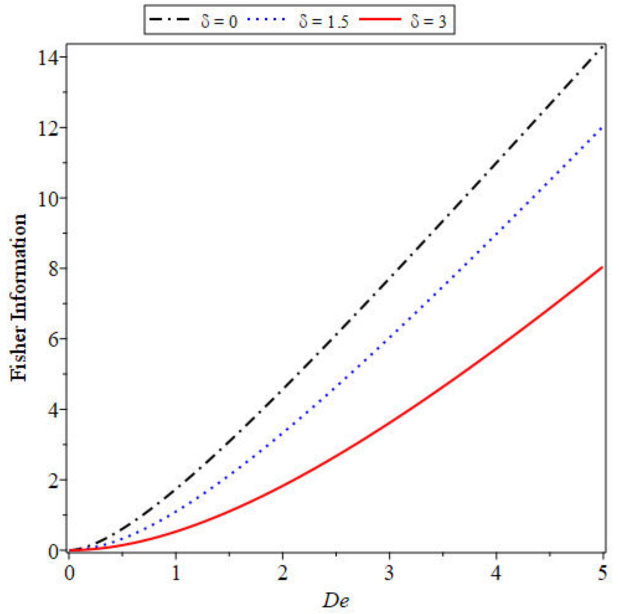

FIGURE 1. Fisher information versus the dissociation energy for $D = 0$, $r_e = 1$ (all quantities are in atomic units), with $n = 2$ and $m = 0$.

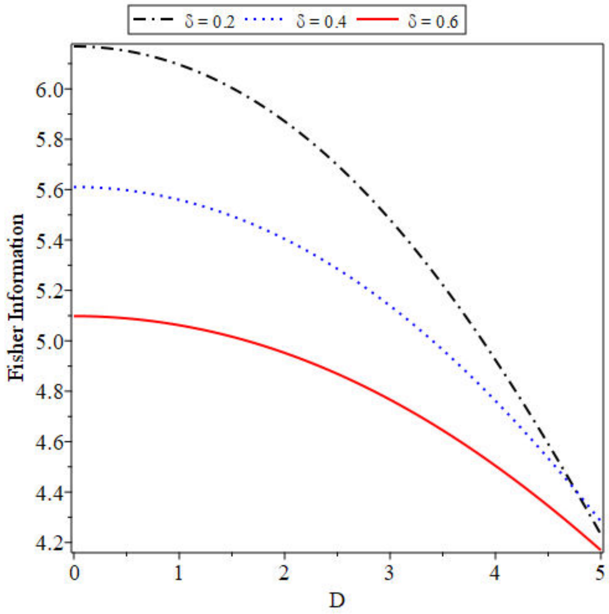

FIGURE 2. Fisher information versus the dipole moment for $De = 3$, $r_e = 1$ (all quantities are in atomic units), with $n = 2$ and $m = 2$.

3.2. Shannon entropy

The Shannon entropy quantifies the uncertainty associated with the localization of a particle in space. Lower entropy values correspond to greater precision in predicting the particle's location. The Shannon information entropy is defined as [55]

$$S(\rho) = -\int \rho(\vec{r})\log\rho(\vec{r})\,d\vec{r} = -\frac{N^2}{4\beta^2}\int_0^{\infty}\int_0^{2\pi} \Phi(\theta)^2 x^{2\lambda} e^{-x}\left[L_n^{2\lambda-1}(x)\right]^2 \log\left[N_r\Phi(\theta)^2 x^{2\lambda-1} e^{-x}\left[L_n^{2\lambda-1}(x)\right]^2\right] dx\,d\theta$$

$$= -\frac{\pi N^2}{4\beta^2}\int_0^{\infty} x^{2\lambda} e^{-x}\left[L_n^{2\lambda-1}(x)\right]^2 \log\left[N^2 x^{2\lambda-1} e^{-x}\left[L_n^{2\lambda-1}(x)\right]^2\right] dx - \frac{I_\theta N^2}{4\beta^2}\int_0^{\infty} x^{2\lambda} e^{-x}\left[L_n^{2\lambda-1}(x)\right]^2 dx, \qquad (31)$$

with $x = 2\beta r$ and

$$I_\theta = \int_0^{2\pi} \Phi(\theta)^2 \log(\Phi(\theta)^2)\,d\theta = \pi\left(1 - 2\log(2)\right), \qquad (32)$$

where the logarithm is taken in base e since we are interested in natural units. The integral (32) is easily obtained for the case of $b = 0$. For $b \neq 0$ one can also show that the integral tends to the same value (32). The integral (31) can be decomposed into four separate integrals

$$S_1 = -\frac{I_\theta N^2}{4\beta^2}\int_0^{\infty} x^{2\lambda} e^{-x}\left[L_n^{2\lambda-1}(x)\right]^2 dx = -\frac{I_\theta}{\pi}. \qquad (33)$$

For the other three integral parts, it is connivent to introduce the orthonormal Laguerre polynomials

$$\tilde{L}_n^{\lambda}(x) = \left[\frac{\Gamma(n+1)}{\Gamma(\lambda+n+1)}\right]^{\frac{1}{2}} L_n^{\lambda}(x), \qquad (34)$$

because they satisfy the simplified orthonormal relation

$$\int_0^{\infty} \tilde{L}_n^{\lambda}(x)\tilde{L}_m^{\lambda}(x) e^{-x} x^{\lambda}\,dx = \delta_{nm}. \qquad (35)$$

TABLE I. Fisher information and Shannon entropy for some diatomic molecules with $\delta = 0.2$, $D = 0.4$ in atomic units.

		Fisher Information			Shannon Entropy		
n	m	$I(Cs_2)$	$I(Li_2)$	$I(SiSn)$	$S(Cs_2)$	$S(Li_2)$	$S(SiSn)$
1	0	1.20	3.01	6.32	6.2815	5.3274	4.6874
	1	1.15	2.86	6.46	6.3875	5.4561	4.7559
	2	1.13	2.75	6.52	6.5810	5.6816	4.8837
2	0	1.39	3.34	8.20	6.9706	6.0591	5.2857
	1	1.32	3.14	7.80	7.0611	6.1641	5.3459
	2	1.25	2.91	7.73	7.2296	6.3581	5.4591
4	0	1.25	2.84	8.11	8.0276	7.1660	6.2181
	1	1.18	2.74	7.84	8.0971	7.2455	6.2676
	2	1.10	2.52	7.61	8.2311	7.3980	6.3601
6	0	0.998	2.27	7.08	8.8416	8.0125	6.9510
	1	0.958	2.17	6.74	8.8981	8.0750	6.9925
	2	0.910	2.01	6.66	9.0096	8.2010	7.0710
8	0	0.798	1.77	5.95	9.5087	8.7020	7.5595
	1	0.770	1.70	5.76	9.5562	8.7525	7.5960
	2	0.733	1.58	5.63	9.6512	8.8600	7.6640

The remaining integrals are then given by

$$S_2 = -\frac{\pi N^2}{4\beta^2}\int_0^\infty x^{2\lambda}e^{-x}\left[L_n^{2\lambda-1}(x)\right]^2 \log\left(N^2\frac{\Gamma(n+2\lambda)}{\Gamma(n+1)}\right)\,dx = -\log\left(\frac{2\beta^2}{(n+\lambda)\pi}\right), \tag{36}$$

$$S_3 = -\frac{\pi N^2}{4\beta^2}\int_0^\infty x^{2\lambda}e^{-x}\left[L_n^{2\lambda-1}(x)\right]^2 \log\left(x^{2\lambda-1}e^{-x}\right)\,dx = \frac{(n+2\lambda)\left[-(2\lambda-1)\Psi(n+2\lambda+1)+2n+2\lambda+1\right]}{2(n+\lambda)}, \tag{37}$$

where $\Psi(z)=\Gamma^{'}(z)/\Gamma(z)$ is the Digamma function [57].

$$\begin{aligned} S_4 &= -\frac{\pi N^2}{4\beta^2}\frac{\Gamma(n+2\lambda)}{\Gamma(n+1)}\int_0^\infty x^{2\lambda}e^{-x}\left[\tilde{L}_n^{2\lambda-1}(x)\right]^2\log\left(\left[\tilde{L}_n^{2\lambda-1}(x)\right]^2\right)\,dx \\ &= -\frac{1}{2(n+\lambda)}\left(-6n^2+4\lambda n\log n+2n\left[\log(2\pi)-4\lambda-2\right]+O(n)\right). \end{aligned} \tag{38}$$

The last integral is derived using the p-norm method [58] at the asymptotic limits. By applying Eqs. (32), (33), and (36)–(38), and simplifying the resulting expression, the Shannon entropy S is given by

$$\begin{aligned} S = \sum_{i=1}^{4} S_i &= 4n+2\lambda-\pi-\ln\left(\frac{\beta^2}{2\pi(n+\lambda)}\right)+\frac{1}{2n+2\lambda} \\ &\times\Big(2n\lambda+5n+1+(1-2\lambda)(n+2\lambda)\Psi(n+2\lambda)-2n\big[2\lambda\ln n+\ln(2\pi)\big]+O(n)\Big). \end{aligned} \tag{39}$$

4. Tsallis and Renyi entropies

The Tsallis entropy is a generalization of the Shannon entropy within the framework of non-extensive statistical mechanics. It is defined as follows [55]

$$T_q = \frac{1}{q-1}\left(1-W_q[\rho]\right), \quad q>0, \quad q\neq 1. \tag{40}$$

The Rényi entropy serves as another extension of the Shannon entropy and is defined as [55]

$$R_q = \frac{1}{1-q}\log\left(W_q[\rho]\right), \quad q>0, \quad q\neq 1, \tag{41}$$

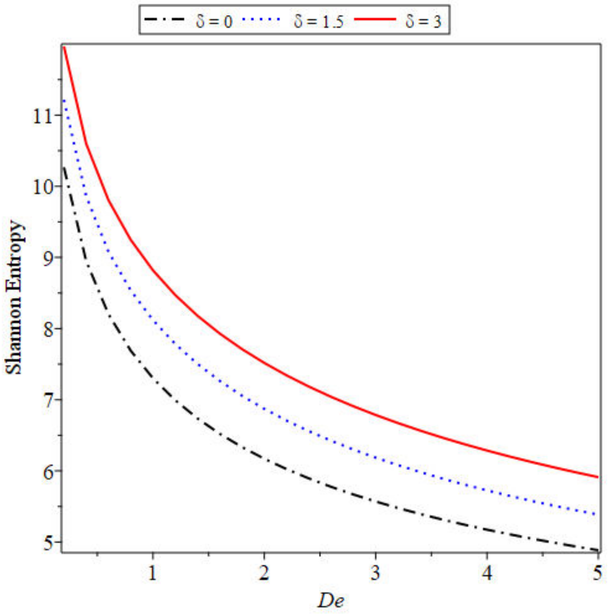

FIGURE 3. Shannon entropy versus the dissociation energy for $D = 0$, $r_e = 1$ (all quantities are in atomic units), with $n = 2$ and $m = 0$.

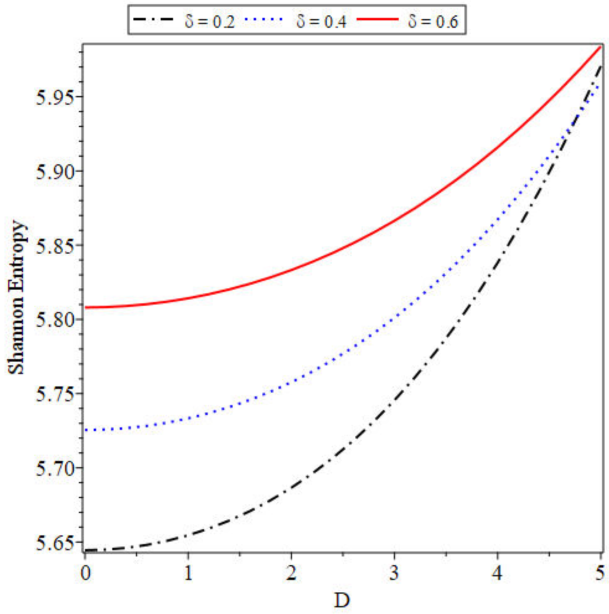

FIGURE 4. Shannon entropy versus the dipole moment for $De = 3$, $r_e = 1$ (all quantities are in atomic units), with $n = 2$ and $m = 2$.

where

$$W_q[\rho] = \int [\rho(\vec{r})]^q \, d\vec{r} = \frac{N^{2q}}{2\beta^2}\frac{(2q-1)!!2\pi}{2^q q!}\int_0^\infty x^{q(2\lambda-1)+1}e^{-qx}\left[L_n^{2\lambda-1}(x)\right]^{2q} dx. \tag{42}$$

In (42) we have used the substitution $x = 2\beta r$ and the fact that

$$\int_0^{2\pi} [\Phi(\theta)]^{2q} \, d\theta = \frac{(2q-1)!!}{2^q q!}2\pi. \tag{43}$$

To evaluate the integral on the right-hand side of Eq. (42) it is useful to employ the linearization formula of Srivastava-Niukkanen for the products of various Laguerre polynomials [59]

$$x^\mu L_{m_1}^{(\alpha_1)}(t_1 x) L_{m_2}^{(\alpha_2)}(t_2 x) \cdots L_{m_r}^{(\alpha_r)}(t_r x) = \sum_{k=0}^{\infty} \gamma_k\left(\mu, \lambda, r, \{m_i\}, \{\alpha_i\}, \{t_i\}\right) L_k^{(\eta)}(x), \tag{44}$$

which is given in terms of the Lauricella's hypergeometric functions of $(r+1)$ variables as

$$\gamma_k\left(\mu, \lambda, r, \{m_i\}, \{\alpha_i\}, \{t_i\}\right) = (\lambda+1)_\mu \binom{\alpha_1 + m_1}{m_1}\binom{\alpha_2 + m_2}{m_2}\cdots$$
$$\cdots\binom{\alpha_r + m_r}{m_r} \times F_A^{(r+1)}\left[\eta+\mu+1, -m_1, \ldots, -m_r, -k; \alpha_1+1, \ldots, \alpha_r+1, \eta+1; t_1, \ldots, t_r, 1\right], \tag{45}$$

where the Pochhammer symbol $(a)_n = \Gamma(a+n)/\Gamma(a)$ and $\binom{\alpha_i + m_i}{m_i}$ are the binomial coefficients. For the special case $(\eta = 0, \ \alpha_1 = \cdots = \alpha_r = 2\lambda - 1, \ m_1 = \cdots = m_r = n, \ x = qt, \ t_1 = \cdots = t_r = 1/q, \ \mu = q(2\lambda-1)+1, \ r = 2q)$ we obtain the linarization

$$(qt)^{q(2\lambda-1)+1}\left[L_n^{(\alpha)}(t)\right]^{2q} = \sum_{k=0}^{\infty}\gamma_k\left(q(2\lambda-1)+1, 0, 2q, \{n\}, \{2\lambda-1\}, \left\{\frac{1}{q}\right\}\right) L_n^{(0)}(qt). \tag{46}$$

The orthogonality property of the polynomial $L_n^{(\alpha)}(x)$ implies that the term with $k = 0$ is the only non-vanishing contribution to the integral (42) [59]. Thus,

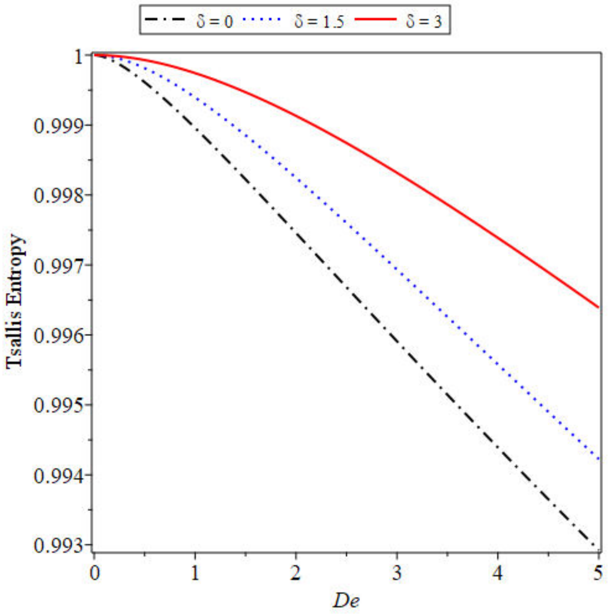

FIGURE 5. Tsallis entropy versus the dissociation energy for $D = 0$, $r_e = 1$ (all quantities are in atomic units), with $n = 2$ and $m = 0$.

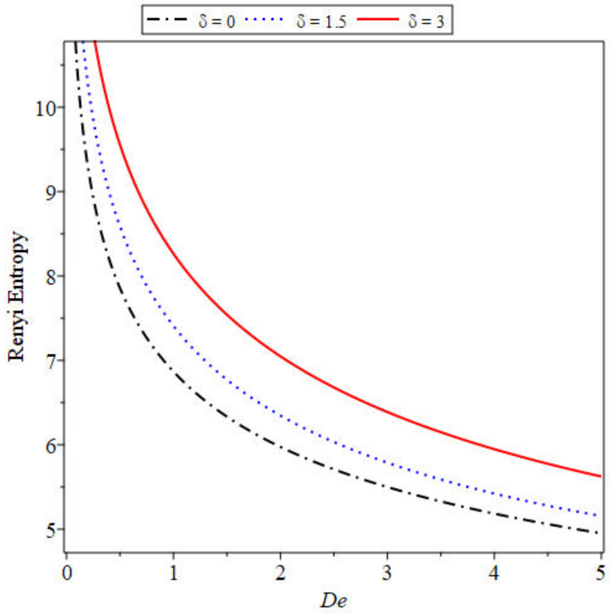

FIGURE 6. Renyi entropy versus the dissociation energy for $D = 0$, $r_e = 1$ (all quantities are in atomic units), with $n = 2$ and $m = 0$.

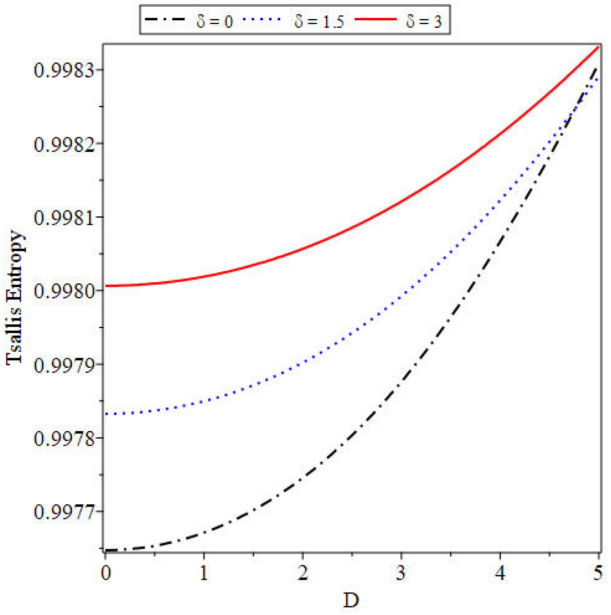

FIGURE 7. Tsallis entropy versus the dipole moment for $De = 3$, $r_e = 1$ (all quantities are in atomic units), with $n = 2$ and $m = 2$.

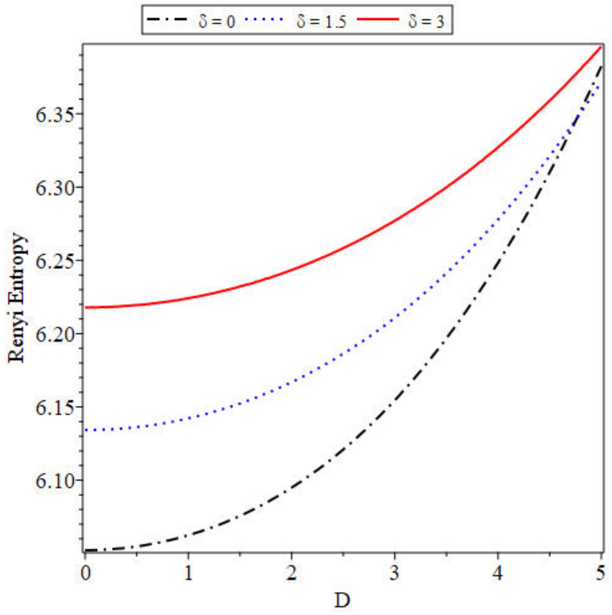

FIGURE 8. Renyi entropy versus the dipole moment for $De = 3$, $r_e = 1$ (all quantities are in atomic units), with $n = 2$ and $m = 2$.

$$\int_0^\infty x^{q(2\lambda-1)+1} e^{-qx} \left[L_n^\alpha(x)\right]^{2q} dx = \frac{1}{q^{q(2\lambda-1)+2}} \gamma_0 \left(q(2\lambda-1)+1, 0, 2q, \{n\}, \{2\lambda-1\}, \left\{\frac{1}{q}\right\}\right), \tag{47}$$

where

$$\begin{aligned}&\gamma_0 \left(q(2\lambda-1)+1, 0, 2q, \{n\}, \{2\lambda-1\}, \left\{\frac{1}{q}\right\}\right) \\ &= \Gamma(q(2\lambda-1)+2) \binom{2\lambda+n-1}{n}^{2q} \times F_A^{(2q+1)} \left[q(2\lambda-1)+2, -n, \ldots, -n, 0; 2\lambda, \ldots, 2\lambda, 1; \frac{1}{q}, \ldots, \frac{1}{q}, 1\right].\end{aligned} \tag{48}$$

TABLE II. Tsallis and the Renyi entropies for some diatomic molecules with $\delta = 0.2, D = 0.4$ in atomic units.

		Tsallis Entropy			Renyi Entropy		
n	m	$T(Cs_2)$	$T(Li_2)$	$T(SiSn)$	$R(Cs_2)$	$R(Li_2)$	$R(SiSn)$
1	0	0.99751	0.99350	0.98784	5.9954	5.0362	4.4098
	1	0.99777	0.99430	0.98866	6.1056	5.1670	4.4792
	2	0.99816	0.99547	0.99003	6.2992	5.3962	4.6084
2	0	0.99876	0.996882	0.99336	6.6897	5.7715	5.0144
	1	0.99887	0.99722	0.99375	6.7849	5.8848	5.0756
	2	0.99904	0.99771	0.99443	6.9526	6.0812	5.1898
4	0	0.99957	0.99898	0.99740	7.7518	6.8894	5.9541
	1	0.99960	0.99907	0.99753	7.8273	6.9778	6.0038
	2	0.99965	0.99920	0.99775	7.9600	7.1311	6.0969
6	0	0.99981	0.99957	0.99876	8.5686	7.7410	6.6907
	1	0.99982	0.99960	0.99881	8.6316	7.8141	6.7326
	2	0.99984	0.99964	0.99890	8.7413	7.9400	6.8115
8	0	0.99990	0.99978	0.99933	9.2367	8.4331	7.3023
	1	0.99991	0.99980	0.99935	9.2909	8.4956	7.3386
	2	0.99992	0.99982	0.99939	9.3847	8.6028	7.4069

Hence

$$W_q[\rho] = \frac{N^{2q}}{2\beta^2}\frac{(2q-1)!!2\pi}{2^q q!}\frac{1}{q^{q(2\lambda-1)+2}}\gamma_0\left(q(2\lambda-1)+1, 0, 2q, \{n\}, \{2\lambda-1\}, \left\{\frac{1}{q}\right\}\right), \tag{49}$$

so that the Tsallis and the Renyi entropies become

$$T_q = \frac{1}{q-1}\left[1 - \frac{N^{2q}}{4\beta^2}\frac{(2q-1)!!2\pi}{2^q q!}\frac{1}{q^{q(2\lambda-1)+2}}\gamma_0\left(q(2\lambda-1)+1, 0, 2q, \{n\}, \{2\lambda-1\}, \left\{\frac{1}{q}\right\}\right)\right], \tag{50}$$

$$R_q = \frac{1}{1-q}\log\left(\frac{N^{2q}}{4\beta^2}\frac{(2q-1)!!2\pi}{2^q q!}\frac{1}{q^{q(2\lambda-1)+2}}\gamma_0\left(q(2\lambda-1)+1, 0, 2q, \{n\}, \{2\lambda-1\}, \left\{\frac{1}{q}\right\}\right)\right), \tag{51}$$

where the normalization constant N is defined by expression (20).

5. Results and discussion

This section is devoted to the discussion of our numerical and graphical results. For convenience, we use the Hartree atomic units defined by $\hbar = e = m_e = 4\pi\epsilon_0 = 1$ (all figures in this article are sketched using atomic units). In Fig. 1 we have examined the effect of dissociation energy D_e on the Fisher information for different values of the AB field parameter δ. First, we mention that the Fisher information is related to the quantum kinetic energy, wherein the kinetic energy is decomposed into classical kinetic energy and purely quantum kinetic energy, with the latter term is the Weizsäcker term, which is essentially identical to the Fisher information [60]. Figure 1 shows that the Fisher information increases with the increasing of the dissociation energy D_e, implying raise in degree of localization. This is obvious since the dissociation energy is amount of energy required to break the bond and separate the combining atoms in the molecule. In the framework of electronic structure dissociation energy connects with the degree of electron localization within the molecule. A higher dissociation energy implies that the bond between the atoms within the molecule is more stronger, which results to electrons being more tightly held between the atoms leading to a higher degree of localization. Moreover, Fig. 1 shows that the Fisher information decreases with the increase of AB field parameter δ, indicating a decrease in localization.

In Fig. 2 we have plotted the Fisher information against the dipole moment terms D for different values of AB field parameter δ. In this figure, and elsewhere when we discuss the impact of dipole moment on different information measures we have to consider the accuracy of the characteristic number of the Mathieu function in Eq. (10). Therefore, we have carefully selected values for the involved parameters to ensure that the characteristic number remains consistent with different leading terms. For $m = 0, 1$, the accuracy of the characteristic number (10) is held for $b < 1$. For $m = 2$, the accuracy can be extended to values of b up to 20. The higher the angular number m, the wider range of b required for the accuracy of the characteristic number. In our case, we choose $m = 2$. Fig. 2 illustrates that increasing the dipole moment and AB field parameter δ leads to a decrease in Fisher information, which results to a loss of information regarding localization.

In Figs. 3 and 4, we have depicted the influence of dissociation energy and dipole moment on the Shannon entropy, respectively. The Shannon entropy gives insights into the precision and spatial localization of particles and it reflects the probability distribution and stability of the system. A lower Shannon entropy indicates greater accuracy in predicting particle localization and, consequently, higher stability. Figure 3 illustrates that dissociation energy reduces Shannon entropy, thereby enhancing precision and spatial localization. This observation aligns with our previous findings, as dissociation energy governs the bond strength between atoms in a molecule. Higher dissociation energy implies tighter electron binding between atoms, leading to increased localization. Figure 4 shows that the dipole moment increases the Shannon entropy and hence decreases the precision and localization as expected. Moreover, akin to the Fisher information scenario, the AB field parameter δ adversely affects the accuracy of particle localization prediction. Shannon entropy increases with δ, resulting in a loss of precision and increased uncertainty regarding particle localization in space as shown in Figs. 3 and 4.

We should note that we have used a numerical method for evaluating and plotting the Shannon entropy in Figs. 3 and 4. The reason for this is that the last integral of the Shannon entropy S_4, Eq. (38), suits high radial numbers since it is calculated in the asymptotic limits [58].

In Figs. 5 and 6, as well as 7 and 8, we investigated the influence of dissociation energy and dipole moment on Tsallis and Renyi entropies, respectively. These entropies are just generalizations of Shannon entropy. Figures 5 and 7 show that the decreasing dissociation energy results in lower Tsallis and Renyi entropies, which results in enhancing precision and spatial localization. Conversely, increasing the dipole moment leads to higher Tsallis and Renyi entropies, thus reducing precision and spatial localization, as depicted in Figs. 6 and 8. Additionally, an increase in the AB field parameter δ leads to a loss in precision and an increase in uncertainty regarding particle localization in space.

Tables I and II demonstrate the numerical analysis of Fisher information and Shannon entropy, the Tsallis and The Renyi entropies, for different eigenstates and some diatomic molecules, namely, SiSn $(X^3\Sigma_g^+ : De = 2.642965641$ eV, $re = 2.514A^0)$, Li$_2(X^1\Sigma_g^+ : De = 1.055918901$ eV, $re = 2.6729A^0)$ and Cs$_2(X^1\Sigma_g^+ : De = 0.4524686595$ eV, $re = 4.648A^0)$ [61, 62] with $q = 2$. It is shown that the Shannon, Tsallis, and Renyi entropies increase with the increase of radial number n_r and angular number m, which means higher accuracy in predicting localization and stability. The Fisher information decreases with the increasing of quantum angular number m, and increases then decreases with the increasing of quantum radial number n_r. The radial number that gives the maximum value to the Fisher information can be rounded analytically or numerically from Eq. (30).

6. Conclusion

In this paper, we first derived the exact analytical solution of the Schrödinger equation for a 2D system subjected to a non-central scalar potential and a vector potential of Aharonov-Bohm (AB) effect and obtained the corresponding wave functions and energy eigenvalues, where the non-central potential is composed of a Kratzer potential plus a dipole moment term. Subsequently, we conducted both analytical and numerical investigations into the information-theoretic measures namely, Fisher information, Shannon entropy, Rényi entropy, and Tsallis entropy.

The analysis of these information-theoretic measures was carried out for various parameters, including the dissociation energy De, the dipole moment D, the AB field parameter δ, as well as the radial and angular quantum numbers for select diatomic molecules. Our findings showed that the Fisher information increases with an increase in dissociation energy De, while it decreases with increasing of dipole moment D, AB field parameter δ, and the radial and angular quantum numbers.

In contrast, the Shannon, Rényi, and Tsallis entropies exhibit a decrease with the rising dissociation energy De, and an increase with decreasing of dipole moment D, AB field parameter δ, and the radial and angular quantum numbers. These observations collectively suggest that higher dissociation energy enhances precision and particle localization in space. Furthermore, our observations indicate that increasing the dipole moment, AB field parameter, and radial and angular quantum numbers reduce the degree of particle localization.

Acknowledgement

This work is supported by PRFU Research Project PRFU B00L02UN050120230005, Univ. Batna1, Algeria.

Compliance with ethical standards

- Conflict of interest: The authors declare that they have no conflict of interest.
- Ethical conduct: This study was carried out following the ethical standards of the journal.

1. T.M. Cover, J.A. Thomas, Elements of Information Theory, 2nd ed. (Wiley-Interscience, New York, 2006), `https://doi.org/10.1002/0471200611`
2. J.B.M. Uffink, Measures of uncertainty and the uncertainty principle, Doctoral dissertation, University of Utrecht (1990).
3. M.J.W. Hall, Universal geometric approach to uncertainty, entropy, and information, *Phys. Rev. A* **59** (1999) 2602, `https://doi.org/10.1103/PhysRevA.59.2602`
4. R.A. Fisher, Theory of Statistical Estimation, *Proc. Cambridge Phil. Soc.* **22** (1925) 700, `https://doi.org/10.1017/S0305004100009580`.
5. B.R. Frieden, Science from Fisher Information, Cambridge University Press, Cambridge (2004), `https://doi.org/10.1017/CBO9780511616907`
6. M.J.W. Hall, Quantum Properties of Classical Fisher Information, *Phys. Rev. A* **62** (2000) 012107, `https://doi.org/10.1103/PhysRevA.62.012107`.
7. M.J.W. Hall, Exact Uncertainty Relations, *Phys. Rev. A* **64** (2001) 052103, `https://doi.org/10.1103/PhysRevA.64.052103`.
8. M. Portes de Albuquerque, I.A. Esquef, and A.R. Gesualdi Mello, Image thresholding using Tsallis entropy, *Pattern Recognition Letters* **25** (2004) 1059, `https://doi.org/10.1016/j.patrec.2004.03.003`
9. O. Sotolongo-Grau, D. Rodriguez-Perez, J.C. Antoranz, O. Sotolongo-Costa, Tissue Radiation Response with Maximum Tsallis Entropy, *Phys. Rev. Lett.* **105** (2010) 158105, `https://doi.org/10.1103/PhysRevLett.105.158105`.
10. R.J.V. dos Santos, Generalization of Shannon's theorem for Tsallis entropy, *J. Math. Phys.* **38** (1997) 4104, `https://doi.org/10.1063/1.532107`
11. J.C. Angulo, J. Antolin, K.D. Sen, Fisher-Shannon plane and statistical complexity of atoms, *Phys. Lett. A* **372** (2008) 670, `https://doi.org/10.1016/j.physleta.2007.07.077`
12. H.E. Montgomery, K.D. Sen, Statistical complexity and Fisher-Shannon information measure of H_2^+, *Phys. Lett. A* **372** (2008) 2271, `https://doi.org/10.1016/j.physleta.2007.11.041`
13. D. Manzano, Statistical measures of complexity for quantum systems with continuous variables, *Physica A* **391** (2012) 6238, `https://doi.org/10.1016/j.physa.2012.06.058`
14. J.C. Angulo, J. Antolín, Atomic complexity measures in position and momentum spaces, *J. Chem. Phys.* **128** (2008) 164109, `https://doi.org/10.1063/1.2907743`
15. R.J. Yáñez, W. Van Assche, J.S. Dehesa, Position and momentum information entropies of the D-dimensional harmonic oscillator and hydrogen atom, *Phys. Rev. A* **50** (1994) 3065, `https://doi.org/10.1103/PhysRevA.50.3065`
16. J.S. Dehesa, S. López-Rosa, B. Olmos, R.J. Yáñez, Fisher information of D-dimensional hydrogenic systems in position and momentum spaces, *J. Math. Phys.* **47** (2006) 052104, `https://doi.org/10.1063/1.2190335`
17. J.S. Dehesa, S. López-Rosa, B. Olmos, R.J. Yáñez, Information measures of hydrogenic systems, Laguerre polynomials and spherical harmonics, *J. Comput. Appl. Math.* **179** (2005) 185, `https://doi.org/10.1016/j.cam.2004.09.040`
18. J.S. Dehesa, A. Martínez-Finkelshtein, V.N. Sorokin, Quantum-information entropies for highly excited states of single-particle systems with power-type potentials, *Phys. Rev. A* **66** (2002) 062109, `https://doi.org/10.1103/PhysRevA.66.062109`
19. E. Romera, P. Sánchez-Moreno, J.S. Dehesa, The Fisher information of single-particle systems with a central potential, *Chem. Phys. Lett.* **414** (2005) 468, `https://doi.org/10.1016/j.cplett.2005.08.032`
20. J.S. Dehesa, A. Martínez-Finkelshtein, V.N. Sorokin, Information-theoretic measures for Morse and Pöschl-Teller potentials, *Molecular Physics* **104** (2006) 613, `https://doi.org/10.1080/00268970500493243`
21. P.A. Bouvrie, J.C. Angulo, J.S. Dehesa, Entropy and complexity analysis of Dirac-delta-like quantum potentials, *Physica A* **390** (2011) 2215, `https://doi.org/10.1016/j.physa.2011.02.020`
22. S. H. Patil, K.D. Sen, Uncertainty relations for modified isotropic harmonic oscillator and Coulomb potentials, *Phys. Lett. A* **362** (2007) 109, `https://doi.org/10.1016/j.physleta.2006.11.045`
23. A. Ghasemi, M.S. Hooshmandasl, M.K. Tavassoly, On the quantum information entropies and squeezing associated with the eigenstates of the isotonic oscillator, *Phys. Scr.* **84** (2011) 035007, `https://doi.org/10.1088/0031-8949/84/03/035007`
24. J.J. Omiste, R.J. Yáñez, J.S. Dehesa, Information-theoretic properties of the half-line Coulomb potential, *J. Math. Chem.* **47** (2010) 911, `https://doi.org/10.1007/s10910-009-9611-8`
25. W.A. Yahya, K.J. Oyewumi, K.D. Sen, Information and complexity measures for the ring-shaped modified Kratzer potential, *Indian J. Chem. A* **53**A (2014) 1307.
26. W.A. Yahya, K.J. Oyewumi, K.D. Sen, Position and momentum information-theoretic measures of the pseudoharmonic potential, *Int. J. Quantum Chem.* **115** (2015) 1543, `https://doi.org/10.1002/qua.24971`
27. C.A. Onate *et al*., Eigen solutions, Shannon entropy and Fisher information under the Eckart Manning Rosen potential model, *J. Korean Phys. Soc.* **70** (2017) 339, `https://doi.org/10.3938/jkps.70.339`
28. C.A. Onate *et al*., Relativistic Treatment of Spin-zero Particles Subjected to the Shifted Tietz-Wei Potential Model, *J. Korean Phys. Soc.* **73** (2018) 531, `https://doi.org/10.3938/jkps.73.531`
29. J.A. Obu, P.O. Okoi, U.S. Okorie, Relativistic and nonrelativistic treatment of Hulthen-Kratzer potential model in D-dimensions, *Indian J. Phys.* **95** (2021) 505, `https://doi.org/10.1007/s12648-019-01638-w`
30. C.A. Onate, A.N. Ikot, M.C. Onyeaju, O. Ebomwonyi, J.O.A. Idiodi, Effect of dissociation energy on Shannon and Rényi entropies, *Karbala Int. J. Mod. Sci.* **4** (2018) 134, `https://doi.org/10.1016/j.kijoms.2017.12.004`

31. A.N. Ikot, G.J. Rampho, P.O. Amadi, U.S. Okorie, M.J. Sithole, M.L. Lekala, Quantum information-entropic measures for exponential-type potential, *Results Phys.* **18** (2020) 103150, `https://doi.org/10.1016/j.rinp.2020.103150`
32. P.O. Amadi, A.N. Ikot, A.T. Ngiangia, U.S. Okorie, G.J. Rampho, H.Y. Abdullah, Shannon entropy and Fisher information for screened Kratzer potential, *Int. J. Quantum Chem.* **120** (2020) e26246, `https://doi.org/10.1002/qua.26246`
33. F. Ayedun, E.P. Inyang, E.A. Ibanga, K.M. Lawal, Analytical solutions to the Schrödinger equation with collective potential models: Application to quantum information theory, *East Eur. J. Phys*. **4** (2022) 87, `https://doi.org/10.26565/2312-4334-2022-4-07`
34. M. Heddar, M. Moumni, M. Falek, Non-Relativistic and Relativistic Equations for the Kratzer Potential plus a Dipole in 2D Systems, *Phys. Scr*. **94** (2019) 125011, `https://doi.10.1088/1402-4896/ab3501`
35. S.M. Ikhdair, An approximate k state solutions of the Dirac equation for the generalized Morse potential under spin and pseudospin symmetry, *J. Math. Phys*. **52** (2011) 052303, `https://doi.org/10.1063/1.3583553`
36. G. Van Hooydonk, Ionic Kratzer bond theory and vibrational levels for achiral covalent bond HH, *Z. Naturforsch. A* **64** (2009) 801.
37. C. Berkdemir, A. Berkdemir, J. Han, Bound state solutions of the Schrödinger equation for modified Kratzer's molecular potential, *Chem. Phys. Lett*. **417** (2006) 326, `https://doi.org/10.1016/j.cplett.2005.10.039`
38. K. Batra, V. Prasad, Spherical quantum dot in Kratzer confining potential: study of linear and nonlinear optical absorption coefficients and refractive index change, *Eur. Phys. J. B* **91** (2018) 298, `https://doi.org/10.1140/epjb/e2018-90432-x`
39. M. Sang, J. Shin, K. Kim, K.J. Yu, Electronic and Thermal Properties of Graphene and Recent Advances in Graphene Based Electronics Applications, *Nanomaterials* **9** (2019) 374, `https://doi.org/10.3390/nano9030374`
40. Y. Du, M. Wang, X. Ye, B. Liu, L. Han, S.H.M. Jafri, W. Liu, X. Zheng, Y. Ning, H. Li, Advances in the Field of Graphene-Based Composites for Energy-Storage Applications, *Crystals* **13** (2023) 912, `https://doi.org/10.3390/cryst13060912`
41. S.S. Bagade, S. Patel, M.M. Malik, P.K. Patel, Recent Advancements in Applications of Graphene to Attain Next-Level Solar Cells, C **9** (2023) 70, `https://doi.org/10.3390/c9030070`
42. S. Dwivedi, Graphene based electrodes for hydrogen fuel cells: A comprehensive review, *Int. J. Hydrogen Energy* **47** (2022) 41848, `https://doi.org/10.1016/j.ijhydene.2022.02.051`
43. F. Xia *et al.*, Black phosphorus and its isoelectronic materials, *Nat. Rev. Phys*. **1** (2019) 306, `https://doi.org/10.1038/s42254-019-0043-5`
44. Z. Wu *et al.*, Large-scale growth of few-layer two-dimensional black phosphorus, *Nat. Mater.* **20** (2021) 1203, `https://doi.org/10.1038/s41563-021-01001-7`
45. S. Manzeli *et al.*, 2D transition metal dichalcogenides, *Nat. Rev. Mater*. **2** (2017) 17033, `https://doi.org/10.1038/natrevmats.2017.33`
46. M. Baazouzi, M. Moumni, M. Falek, Exact solutions for a quantum ring with a dipolar impurity, *Eur. Phys. J. Plus* **135** (2020) 894, `https://doi.org/10.1140/epjp/s13360-020-00922-7`
47. M. Abramowitz and I.A. Stegun, Handbook of Mathematical Functions (Dover Publ., New York, 1972).
48. https://dlmf.nist.gov/28.6 (2018-12-15)
49. N.R. Jazar, Mathieu equation, in Approximation Methods in Science and Engineering, (Springer, New York, NY, 2020).
50. D. Frenkel and R. Portugal, Algebraic methods to compute Mathieu functions, *J. Phys. A* **34** (2001) 3541, `https://doi.org/10.1088/0305-4470/34/17/302`
51. M. Gadella, J. Negro, L.M. Nieto, G.P. Pronko, Two Charged Particles in the Plane Under a Constant Perpendicular Magnetic Field, *Int. J. Theor. Phys*. **50** (2011) 2019, `https://doi.org/10.1007/s10773-010-0539-3`
52. D. Zwillinger and V. Moll, editors, Table of Integrals, Series, and Products, 8th ed., originally by I.S. Gradshteyn and I.M. Ryzhik, (Academic Press 2014).
53. G. Casella and R. L. Berger, Statistical Inference, (Duxbury Press 2002).
54. J. J. Sakurai and J. S. Napolitano, Modern Quantum Mechanics, (Cambridge University Press 2017).
55. D. Chakraborty and P. W. Ayers, Statistical Complexity: Applications in Electronic Structure, (edited by K. D. Sen, Springer 2012).
56. M. M. Nieto and L. M. Simmons, Eigenstates, coherent states, and uncertainty products for the Morse oscillator, *Phys. Rev. A* **19** (1979) 438, `https://doi.org/10.1103/PhysRevA.19.438`
57. J. Sánchez-Ruiz and J. Dehesa, Entropic integrals of orthogonal hypergeometric polynomials with general supports, *J. Comput. Appl. Math.* **118** (2000) 311, `https://doi.org/10.1016/S0377-0427(00)00296-X`
58. J. S. Dehesa, R. J. Yáñez, A. I. Aptekarev, and V. Buyarov, Strong asymptotics of Laguerre polynomials and information entropies of two-dimensional harmonic oscillator and one-dimensional Coulomb potentials, *J. Math. Phys*. **39** (1998) 3050, `https://doi.org/10.1063/1.532238`
59. P. Sánchez-Moreno, D. Manzano, and J. S. Dehesa, Direct Spreading Measures of Laguerre Polynomials, *J. Comput. App. Math*. **235** (2011) 1129, `https://doi.org/10.1016/j.cam.2010.07.022`
60. I. P. Hamilton and R. A. Mosna, Fisher information and kinetic energy functionals: A dequantization approach, *J. Comput. App. Math*. **233** (2010) 1542, `https://doi.org/10.1016/j.cam.2009.02.087`
61. A. Ciccioli, G. Gigli, G. Meloni, E. Testani, The dissociation energy of the new diatomic molecules SiPb and GePb, *J. Chem. Phys.* **127** (2007) 054303, `https://doi.org/10.1063/1.2752803`
62. S. Kaur, C. G. Mahajan, Dissociation energy of diatomic molecules, *Pramana. J. Phys.* **50** (1998) 397, `https://doi.org/10.1007/BF02847369`.